

Article

Tensile Strength and Mode I Fracture Toughness of Polymer Concretes Enhanced with Glass Fibers and Metal Chips

Mazaher Salamat-Talab ¹, Ali Zeinolabedin-Beygi ², Faraz Soltani ³, Alireza Akhavan-Safar ^{4,*}, Ricardo J. C. Carbas ^{4,*} and Lucas F. M. da Silva ⁵

¹ Department of Mechanical Engineering, Arak University of Technology, Arak 3818146763, Iran; m.salamattalab@gmail.com

² Department of Mechanical Engineering, Tarbiat Modares University, Tehran 1411713116, Iran; alizeynolabedin8@gmail.com

³ Department of Mining Engineering, Arak University of Technology, Arak 3818146763, Iran; faraz.soltani@arakut.ac.ir

⁴ Institute of Science and Innovation in Mechanical and Industrial Engineering (INEGI), 4200-465 Porto, Portugal

⁵ Department of Mechanical Engineering, Faculty of Engineering, University of Porto, 4200-465 Porto, Portugal; lucas@fe.up.pt

* Correspondence: aakhavan-safar@inegi.up.pt (A.A.-S.); rcarbas@fe.up.pt (R.J.C.C.)

Abstract: This study experimentally investigates the influence of metal chips and glass fibers on the mode I fracture toughness, energy absorption, and tensile strength of polymer concretes (PCs) manufactured by waste aggregates. A substantial portion of the materials employed in manufacturing and enhancing the tested polymer concrete are sourced from waste material. To achieve this, semi-circular bend (SCB) samples were fabricated, both with and without a central crack, to analyze the strength and fracture behavior of the composite specimens. The specimens incorporated varying weight percentages comprising 50 wt% coarse mineral aggregate, 25 wt% fine mineral aggregate, and 25 wt% epoxy resin. Metal chips and glass fibers were introduced at 2, 4, and 8 wt% of the PC material to enhance its mechanical response. Subsequently, the specimens underwent 3-point bending tests to obtain tensile strength, mode I fracture toughness, and energy absorption up to failure. The findings revealed that adding 4% brass chips along with 4% glass fibers significantly enhanced energy absorption (by a factor of 3.8). However, using 4% glass fibers alone improved it even more (by a factor of 10.5). According to the results, glass fibers have a greater impact than brass chips. Introducing 8% glass fibers enhanced the fracture energy by 92%. However, in unfilled samples, aggregate fracture and separation hindered crack propagation, and filled samples presented added barriers, resulting in multiple-site cracking.

Keywords: polymer concrete; glass fibers; metal chips; semi-circular bend; fracture energy; tensile strength



Citation: Salamat-Talab, M.; Zeinolabedin-Beygi, A.; Soltani, F.; Akhavan-Safar, A.; Carbas, R.J.C.; da Silva, L.F.M. Tensile Strength and Mode I Fracture Toughness of Polymer Concretes Enhanced with Glass Fibers and Metal Chips. *Materials* **2024**, *17*, 2094. <https://doi.org/10.3390/ma17092094>

Academic Editors: Jiaqing Wang, Fangyuan Gong, Shuaicheng Guo, Ruizhe Si and Chaochao Liu

Received: 9 March 2024

Revised: 26 April 2024

Accepted: 27 April 2024

Published: 29 April 2024



Copyright: © 2024 by the authors. Licensee MDPI, Basel, Switzerland. This article is an open access article distributed under the terms and conditions of the Creative Commons Attribution (CC BY) license (<https://creativecommons.org/licenses/by/4.0/>).

1. Introduction

Different types of concrete materials, which are usually a mixture of adhesives, aggregates, and sometimes reinforcements, are used in the construction of structures. The advantages of concrete materials include ease of use, low cost, and high compressive strength. However, they have disadvantages such as high porosity, poor tensile strength, chemical corrosion, and high sensitivity to environmental conditions [1]. Various authors have explored composite concretes [2,3]. Nevertheless, within the realm of composite concretes, those composed of materials, specifically polymer concretes, have garnered comparatively limited research attention. Polymer concrete (PC) is produced from a mixture of mineral aggregates with polymer adhesives, which is relatively newer compared to conventional cement concrete materials [4,5]. Additives, polymers and aggregates are used

in making polymer concrete materials [6]. Generally, large and small aggregates constitute more than 75–80% of PC materials. Epoxy and polyester resins can be referred to as common matrix in polymer concrete materials. In addition, different types of fillers are added to the matrix and aggregates to improve the mechanical properties and performance of these materials [7,8]. The advantages of PC materials include high corrosion resistance, good resistance to chemical reactivity, preservation of concrete against carbonation phenomena, and ease of use in thin sections [9,10]. Although PC materials are more expensive than common concrete, their use is useful for stabilizing existing structures. Experimental studies have shown that the fracture energy and tensile strength of PC materials is 3.5–4.5 times that of conventional cement concrete structures, so they can be considered as a suitable alternative to cement concrete [11,12].

In general, three methods of changing the portion of concrete elements, changing the type of resin, and adding fillers are used to increase the mechanical performance of PCs. Considering the expensiveness of resins that have high mechanical properties, changing the type of resin is not a cost-effective method. Regarding the method of changing the percentage of concrete elements, the reduction of resin leads to concrete drying and the increase of resin also reduces some mechanical properties. Several studies have been conducted to achieve the optimal combination of PC materials to achieve good mechanical properties [13,14]. One simple method to improve the mechanical behavior of PC materials is to add filler, with the cost of this method depending on the type of filler. For example, waste material has a much lower price compared to nanoparticles. Many researchers have used waste material to increase mechanical properties [15–21]. Therefore, to increase the mechanical properties of polymer concrete materials, various waste materials have been used [22,23]. Son and Yeon [24] investigated the effect of methacrylic acid filler on the mechanical behavior of polymer material at low temperatures. The results showed that the addition of methacrylic acid increases Poisson's ratio, tensile strength, and Young's modulus of PC. D'Alessandro et al. [25] calculated the thermal conductivity and dynamic stiffness of concrete containing polymers made by electric wire sheets. They found that improved PC can be used for acoustic and thermal coatings of lightweight insulation. Kou and Poon [26] observed that adding fly ash as a filler to the polymer mixture improves chemical resistance with greater flexibility. The effect of burning wood ash as a filler on the mechanical performance of PCs was investigated by Teixeira et al. [27]. They found that the addition of wood ash increases the durability, while it has a detrimental effect on the mechanical properties. The effect of incorporating electronic plastic waste on the mechanical behavior of PC was investigated by Bulut and Şahin [28]. The results showed that by adding filler, compressive strength and bending strength decrease, but ductility increases. Heidari-Rarani et al. [29] investigated the mode I fracture toughness and tensile strength of an optimized epoxy PC using three different freeze/thaw cycles. For this purpose, they used single edge notch bending (SENB) and Brazilian disk (BD) samples. They found that the mode I fracture toughness and tensile strength of PC materials increase significantly with the heat-to-cool thermal cycle. In addition, it was found that an increase in the average temperature of the thermal cycles leads to a decrease in the mode I fracture toughness and tensile strength. Aliha et al. [30] investigated the effect of large silica aggregate mix-design made of epoxy resin, E-glass fibers, and small sand filler on mode I cracking behavior using semi-circular bend (SCB) samples. The results showed that the mechanical performance of PC mix is not always improved by adding fiber to particular mix-designs. In addition, it was shown that the fracture energy and mode I fracture toughness in some cases of PC mix-design (PC with 2% short glass fibers) increased up to 53 and 41%. Asdollah-Tabar et al. [31] investigated the fracture energy and mode I fracture toughness of the PC material by adding recycled polyethylene terephthalate (PET) bottles. For this purpose, two different sizes were used. They found that the fracture toughness of the PC material increased by approximately 16% with the addition of coarse PET filler. Also, if a large PET filler is used, the mode I fracture toughness can be significantly increased compared to the addition of a small PET filler.

As mentioned, many of the studies focused on improvement mechanical performance of PCs and no comprehensive study was made on the effect of brass metal chips and mixture of metal chips with glass fibers on the tensile strength and mode I fracture toughness of PCs. Therefore, this study aims to manufacture PC materials using waste mineral aggregates and two types of fillers, and to investigate their tensile strength and mode I fracture behavior experimentally. For this purpose, glass fibers and brass chips, which are the rounding out of the machining process, were used in different weight percentages (2 wt%, 4 wt%, and 8 wt%). Fracture and 3-point bending (3PB) tests were then performed with and without central crack SCB samples to obtain the mode I fracture toughness, tensile strength, and energy absorbed until failure.

2. Experimental Procedure

2.1. Sample Configuration and Material

Generally, epoxy and polyester resins are used to make PC, and epoxy resins are more common in the industry due to easier control of gel time and better material properties than polyester resin [32]. For this purpose, EPL 1012 epoxy resin was used together with EPH 112 hardener, with a weight ratio of 100:12 [33,34]. Table 1 shows the mechanical properties of EPL 1012 resin and EPH 112 hardener. The weight percentage of the resin used was 25 wt%. To complete the curing and obtain maximum strength, this resin was post-cured at room temperature for 7 days. The polyester resin used in this study was obtained from the Boytec company (Istanbul, Turkey) and was polymerized by adding 0.6 wt% hardener (methyl ethyl ketone peroxide). The resin was cured at room temperature for 40 h and, finally, according to the producer's instructions, the sample was placed in the oven for 8 h at a temperature of 80 °C for post-curing [35].

Mineral aggregates (quartz) in different diameters and with constant grain size are used in PC materials. The advantages of these wasted mineral aggregates include great bonding to polymers and high compressive strength. In Table 2, the chemical composition of this type of aggregate is presented. It should be noted that in order to remove the natural oil and wax that covers the surface of the mineral aggregates, before using them, their surface was treated and they were placed under a temperature of 100 °C for 3 h to dry. According to a previous study [36], aggregates with different weight percentages and sizes (including 50 wt% with 2–4 mm, 20 wt% with 150 µm–2 mm, and 5 wt% under 150 µm) were used to manufacture the samples. Figure 1 shows the different sizes of the aggregates used in this study. To increase the mechanical properties and improve the performance of PC materials, glass fibers and metal chips obtained from the machining process [37] were used. The metal chips used in this study were brass, and they were cleaned with acetone and cured at 50 °C for 30 min. Glass fiber was used from the composite sample that was made in advance. It is worth mentioning that if high-viscosity resin was utilized to manufacture the PC, the ingredients, particularly chopped glass fiber or aggregates, may be agglomerated. Therefore, in this study, low-viscosity (900–1100 cP at 25 °C) resin was used. In addition, in order to have a uniform mixture, all ingredients with their weight fractions were mixed inside a container using a mechanical stirrer for 5 min.

Table 1. Mechanical properties of EPL 1012 and EPH 112 [38].

Tensile Strength (kgf/cm ²)	761
Tensile Modulus (kgf/cm ²)	27,890
Flexural Strength (kgf/cm ²)	960
Flexural Modulus (kgf/cm ²)	36,454
Shore Hardness	82
Viscosity at 25 °C (mPa.s)–EPL 1012	900–1100
Viscosity at 25 °C (mPa.s)–EPH 112	30

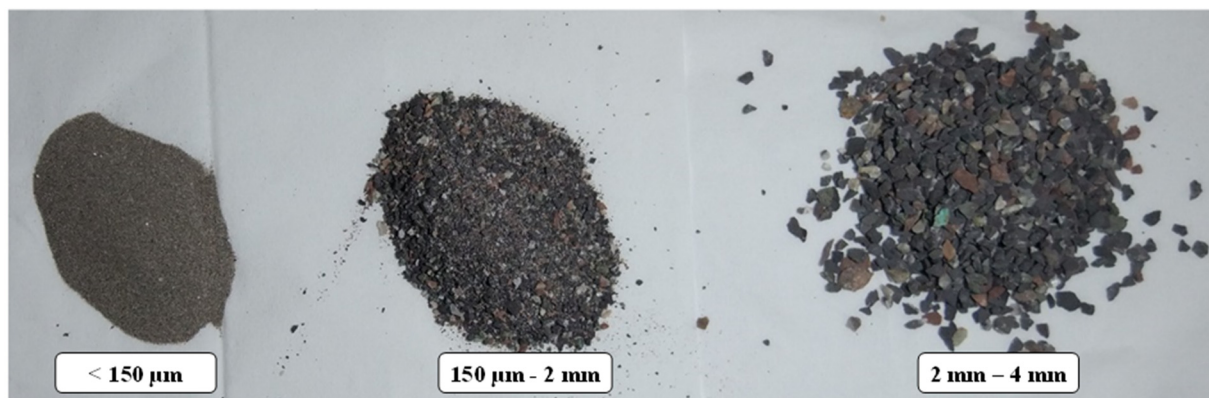


Figure 1. Wasted mineral aggregates in different sizes.

Table 2. Chemical compounds of mineral aggregates [32].

Compounds	wt%
SiO ₂	97.5
Fe ₂ O ₃	0.85
Al ₂ O ₃	0.95
K ₂ O	0.19
CaO	0.27
MgO	0.24

2.2. Sample Geometry and Test Conditions

Researchers have used samples with different geometries for fracture and strength tests on PCs [39–44]. In this study, SCB samples were used to obtain the mode I fracture toughness, energy absorbed until failure, and tensile strength of PC materials. SCB samples were made from a mixture of epoxy resin, waste mineral aggregates, and fillers (brass chips and glass fibers). Figure 2 shows the circular molds used to manufacture the samples, which were created from PVC pipe cuts. Samples with a diameter of 105 mm and thicknesses of 30 mm and 22 mm were used for fracture and strength tests, respectively. An edge pre-crack was created by using an aluminum sheet with a thickness of 0.3 mm. The ratio of the crack length to the radius of the specimen was considered as 0.4. After one day, the specimens were taken out from the mold. The samples were then cured at 90 °C for 2 h. It should be noted that the samples were kept at room temperature for 7 days before the experiment. SCB samples with pre-crack were used for the fracture test and samples without cracks were used for the strength analysis. Figure 3 shows the test specimens. Table 3 also shows the details of the ingredients of the samples. For each condition, three samples were manufactured and tested.

Table 3. Weight percentage of the components used in PC materials.

Sample Configuration	Mineral Aggregate (wt%)	Epoxy Resin (wt%)	Glass Fiber (wt%)	Brass Chip (wt%)
PC–No additive	75	25	0	0
Br (2 wt%)	73	25	0	2
Br (1 wt%) and Fiber (1 wt%)	73	25	1	1
Fiber (2 wt%)	73	25	2	0
Br (4 wt%)	72	24	0	4
Br (2 wt%) and Fiber (2 wt%)	72	24	2	2
Fiber (4 wt%)	72	24	4	0
Br (8 wt%)	70	22	0	8
Br (4 wt%) and Fiber (4 wt%)	70	22	4	4
Fiber (8 wt%)	70	22	8	0

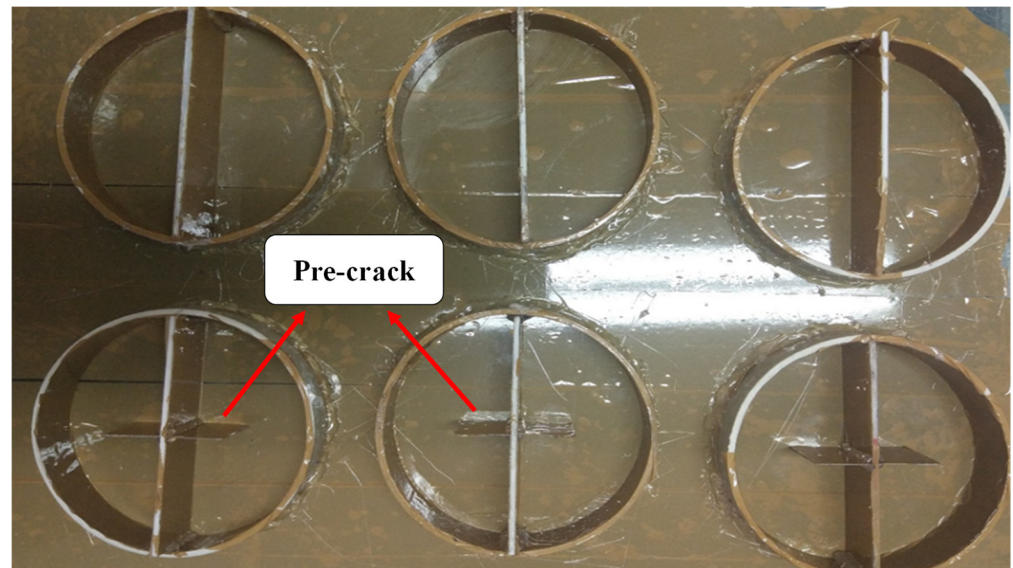


Figure 2. Circular molds used to make SCB specimens.

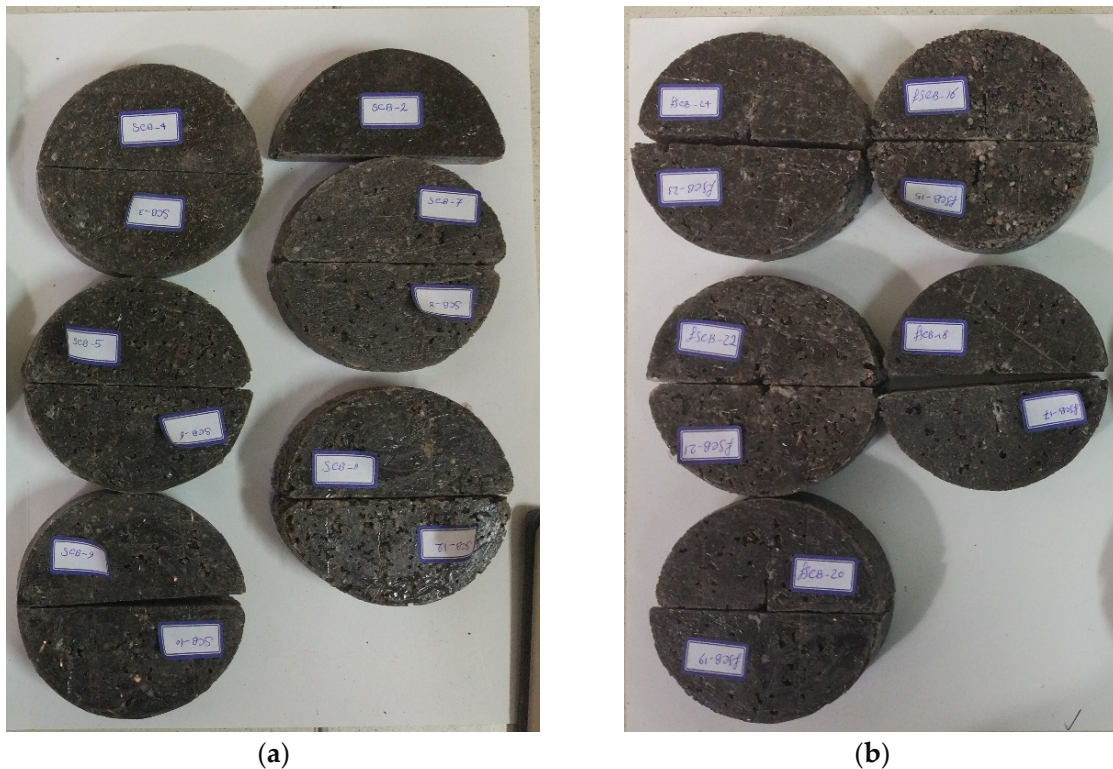


Figure 3. SCB samples with and without pre-crack for (a) strength and (b) fracture tests.

2.3. Data Reduction Approach

An STM-150 universal test machine (Santam company, Tehran, Iran), with a capacity of 250 kN, was used for fracture and strength tests to obtain load–displacement curves of the specimens. It should be noted that the type of loading was displacement control and a speed of 0.5 mm/min was used [45]. The test setup and specimen under load are shown in Figure 4. The tensile strength was obtained from Equation (1) [11]:

$$\sigma_t(\text{SCB}) = \frac{P_f}{\pi t R} \left[0.073 \left(\frac{t}{R} \right) - 0.8896 \right] \left[2.01 \left(\frac{S}{R} \right) + 1.052 \right] \quad (1)$$

where P_f and t are the maximum fracture load and thickness for the SCB specimen, respectively, S is the span length, and R is the radius of the specimens. To obtain the energy absorbed until failure, the area under the load–displacement curve of each test was calculated. Using Equation (2), the amount of absorbed energy can be extracted using the equation below:

$$J_f = \int_0^{\Delta u} P \cdot du \quad (2)$$

where P is the applied load, J_f is the energy absorbed until failure, and u is the displacement measured by the testing machine.

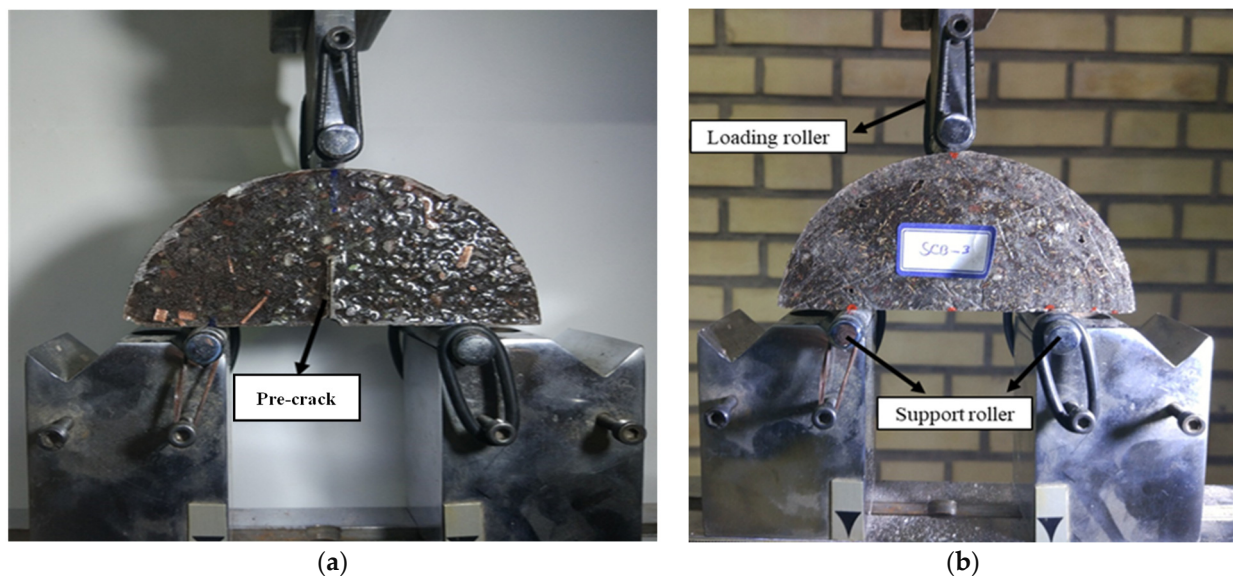


Figure 4. Test setup for (a) fracture test and (b) strength test (with no pre-crack).

The fracture load in each of the samples was obtained by the test. Using Equation (3), the mode I fracture toughness value (K_{IC}) can be determined [46]:

$$K_{IC} = \frac{P_c \sqrt{a}}{RB \sqrt{\pi}} Y_I(a, R) \quad (3)$$

where P_c is the fracture load, R is the disc radius, B is the sample thickness, a is half the length of the crack, and Y_I is the geometric factor for mode I loading of SCB specimens, which is a function of the crack length-to-radius ratio. In this study, in order to determine the geometric factor for the tested setting, the figures reported by Ayatollahi and Aliha [46] were used. According to the mentioned explanations, by using the size of SCB samples (Section 2.2) and the fracture load obtained from the experimental tests, the fracture toughness of the samples was obtained.

3. Results and Discussion

To select one of the resins considered in this study, SCB PCs without fillers were made using two matrices, epoxy and polyester. The tensile strength of neat epoxy and polyester are 74.6 MPa and 25.5 MPa, respectively [38,47]. Therefore, in the following, the PCs manufactured by two different matrices were analyzed in terms of strength and fracture toughness. In other words, the polymer concrete samples in this section have 75% mineral aggregates and 25% matrix; in one of the samples, epoxy was used as matrix, and in the other sample, polyester was used as matrix. Figure 5 shows typical load–displacement curves for each condition. In these curves, displacement was measured by the testing machine. Based on Figure 6, it is evident that the tensile strength of the PC made by the

epoxy matrix is greater than that made by the polyester matrix. However, the fracture toughness values for both matrices are approximately equal. Additionally, it is important to mention that the epoxy resin has a longer gel time compared to the polyester matrix. The polyester matrix has a gel time of less than 10 min, which is unsuitable for fabricating PC specimens. Consequently, epoxy resin was chosen for the manufacture of the PC samples.

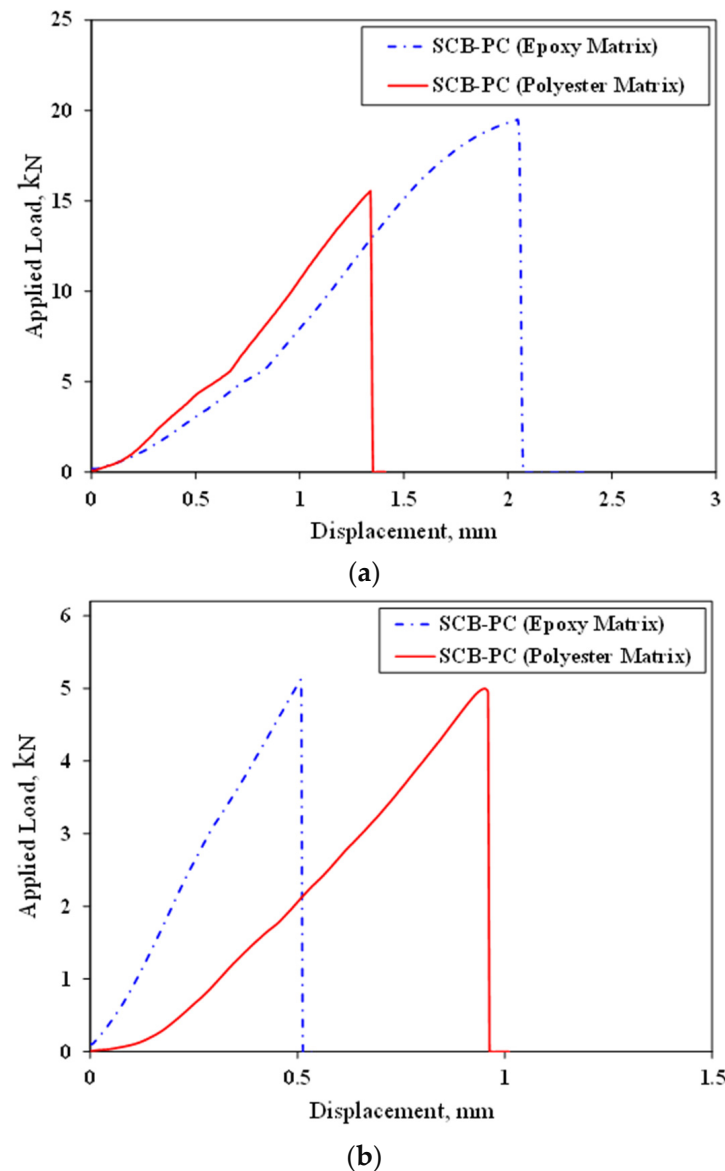


Figure 5. Typical load–displacement curves obtained for polymer concrete samples manufactured using two different resins: (a) strength and (b) fracture tests.

3.1. Tensile Test Results

Figure 7 shows the typical load–displacement curves and tensile strength of PC with 4 wt% additives (different combinations). As shown, by adding brass chips and glass fibers, the tensile strength of the PC material does not change significantly. It should be noted that the reference legend in the following figures refers to PC manufacture by 75 wt% mineral aggregates and 25 wt% epoxy as matrix that does not contain any additives. Figure 8 shows the fracture surface of the tested samples. As crack growth is a gradual process, it does not break upon encountering the fibers. Instead, the matrix cracks elsewhere, resulting in a crack-arresting phenomenon.

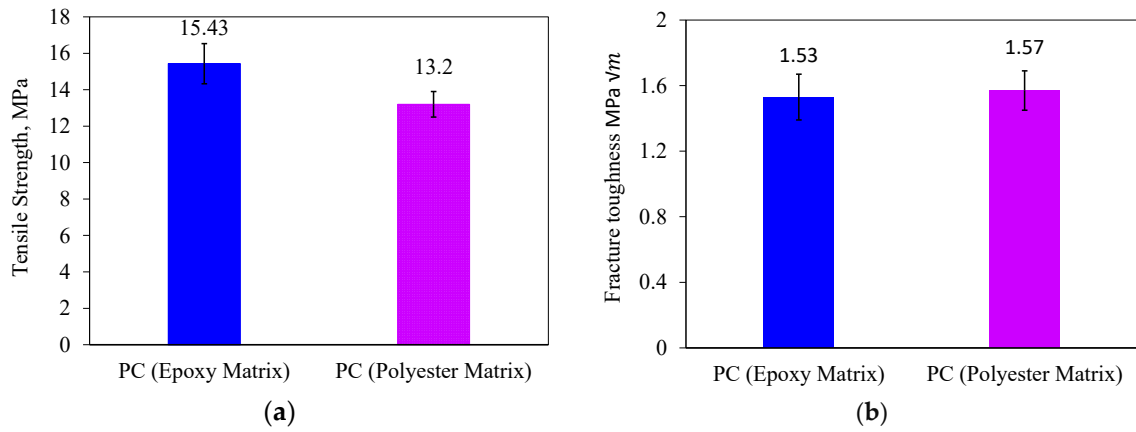


Figure 6. Tensile strength (a) and fracture toughness (b) of polymer concrete samples manufactured with two different matrices.

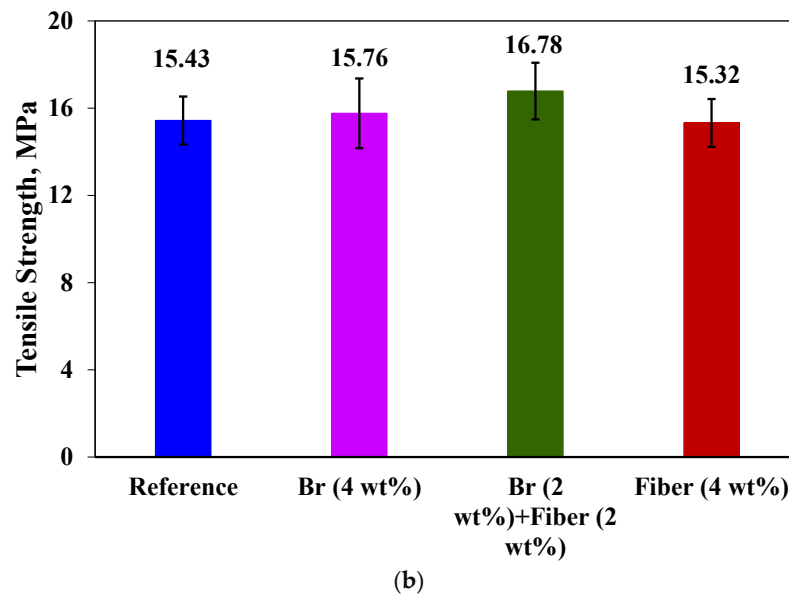
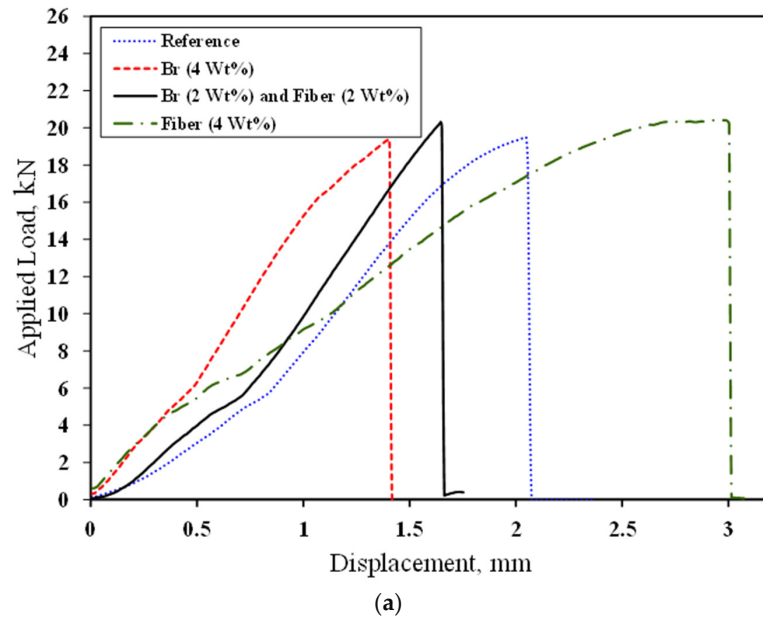


Figure 7. Load–displacement curves (a) and tensile strength (b) of SCB specimens.

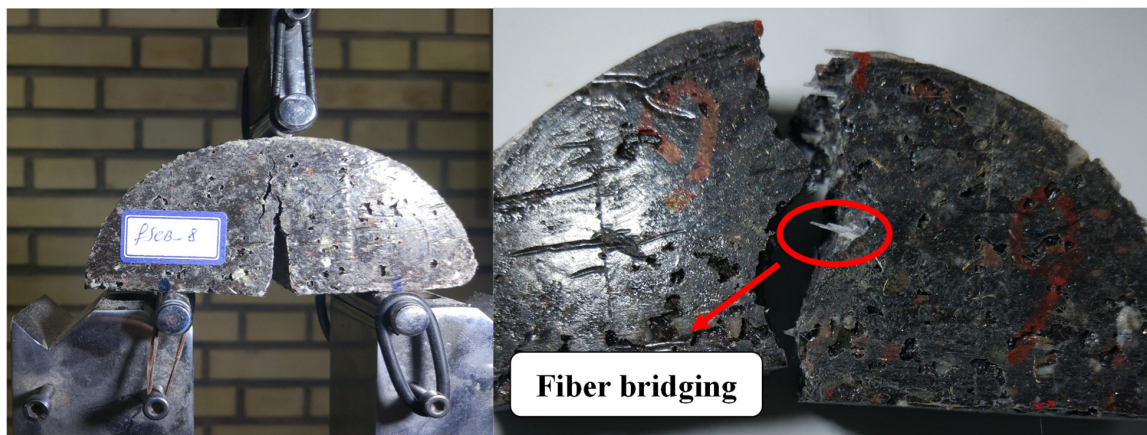


Figure 8. PC samples during the test and after fracture.

3.2. Absorbed Energy

Figure 9 shows the average energies obtained for samples with 2 wt%, 4 wt%, and 8 wt% additives. The highest absorbed energy until failure was obtained for PC with 4 wt% and 8 wt% glass fibers, as shown in Figure 9. The bridging mechanism observed in the specimens can be attributed to the increased energy absorption in the PC material. This phenomenon is a result of the addition of metal chips and glass fibers, which prevent rapid crack growth and resist it. Consequently, this factor contributes to an increase in absorbed energy.

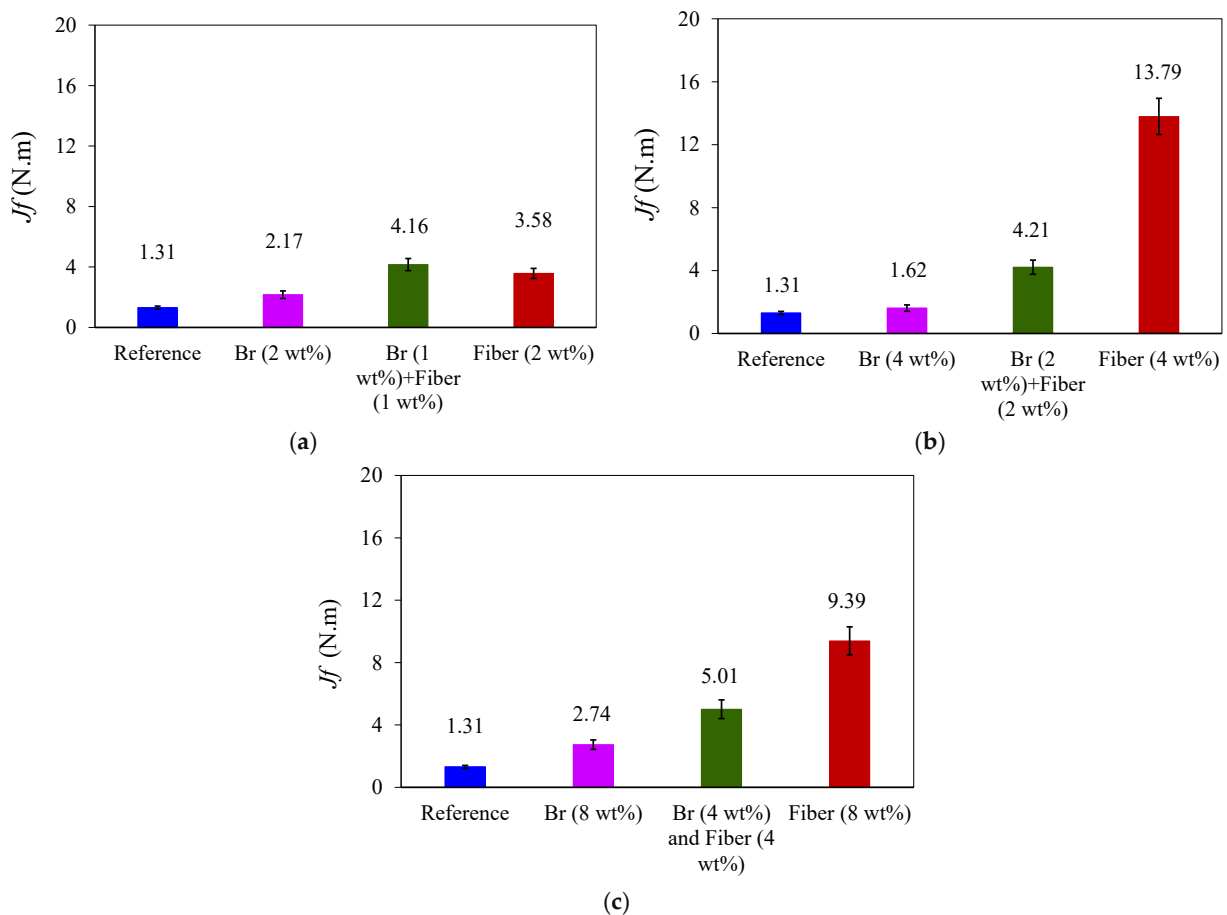
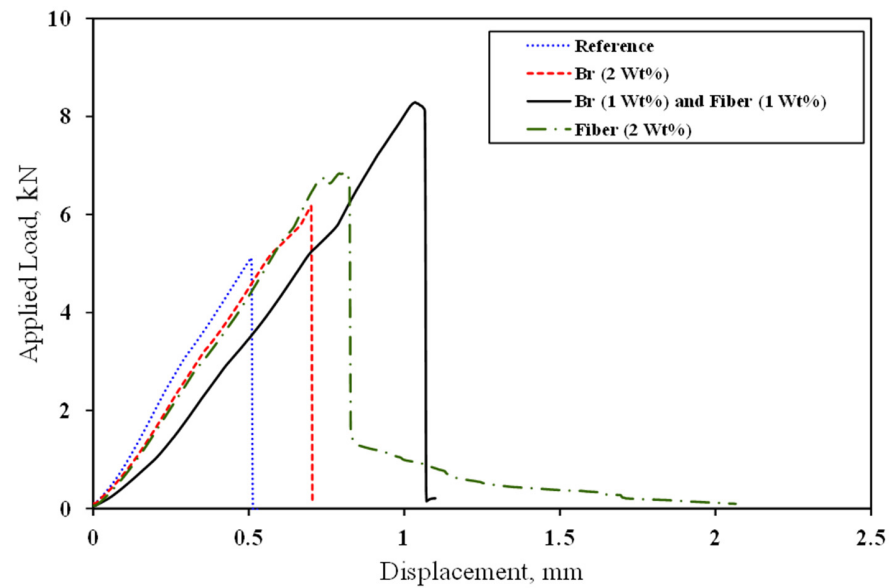


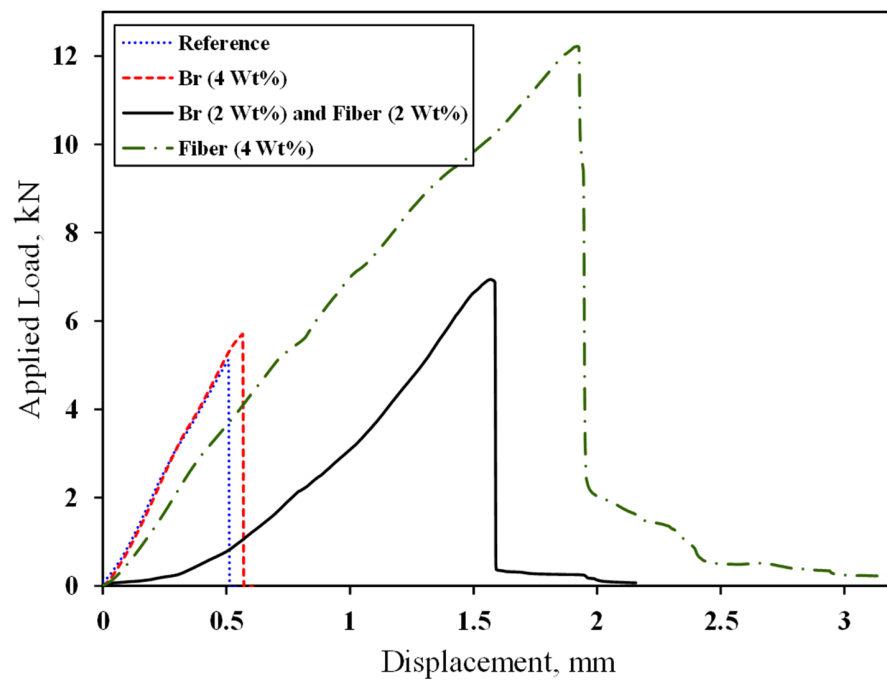
Figure 9. Average absorbed energy until the failure of SCB specimens for samples with (a) 2 wt%, (b) 4 wt%, and (c) 8 wt% additives.

3.3. Fracture Toughness

To assess the mode I fracture toughness, we conducted mode I fracture tests on SCB samples containing initial pre-cracks. It is important to highlight that in all the samples, failure originated from the crack tip. Figure 10 illustrates the load–displacement curves for samples with varying weight ratios of fillers, including 2 wt%, 4 wt%, and 8 wt%. Table 4 displays the maximum load and maximum displacement at failure in fracture tests. Notably, the sample containing 4 wt% fiber exhibited a significant improvement, with a 139% increase in maximum load and a remarkable 578% increase in displacement at the point of final failure. It is worth mentioning the gradual failure observed in the SCB samples, which effectively mitigates abrupt failure.



(a)



(b)

Figure 10. Cont.

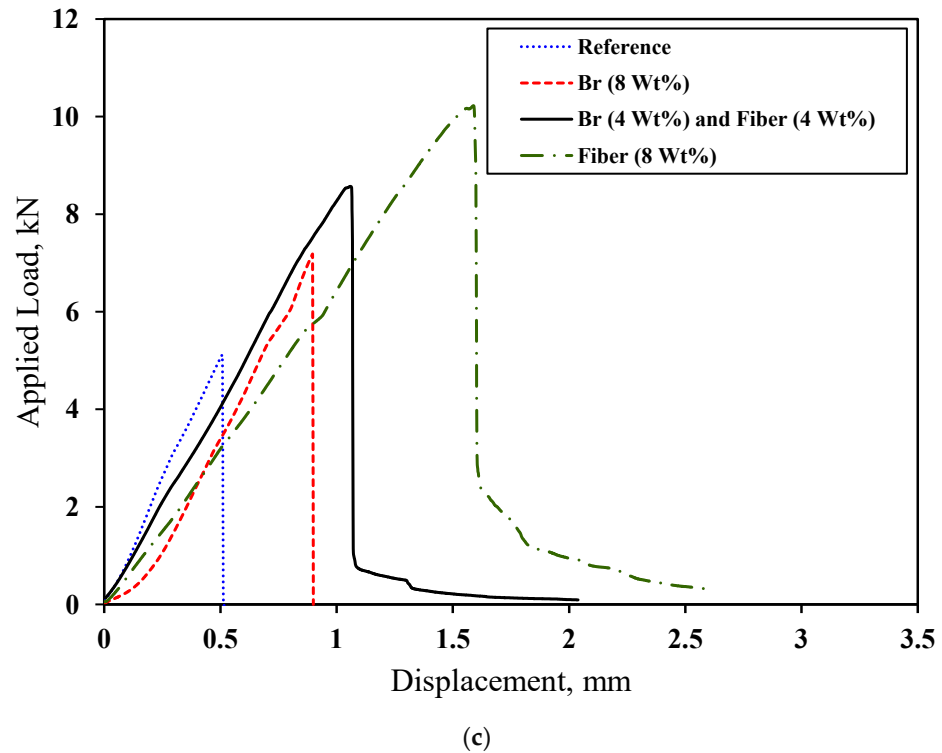
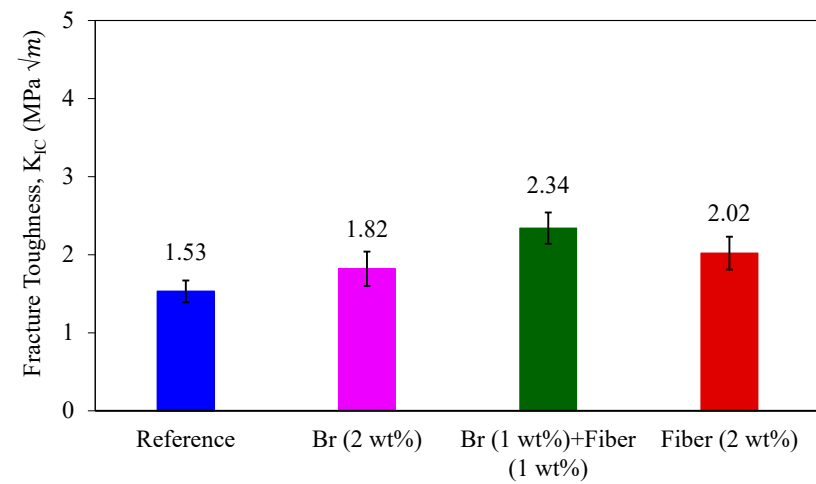


Figure 10. Load–displacement curves obtained for SCB samples with central crack in the states of (a) 2 wt%, (b) 4 wt%, and (c) 8 wt% under fracture test.

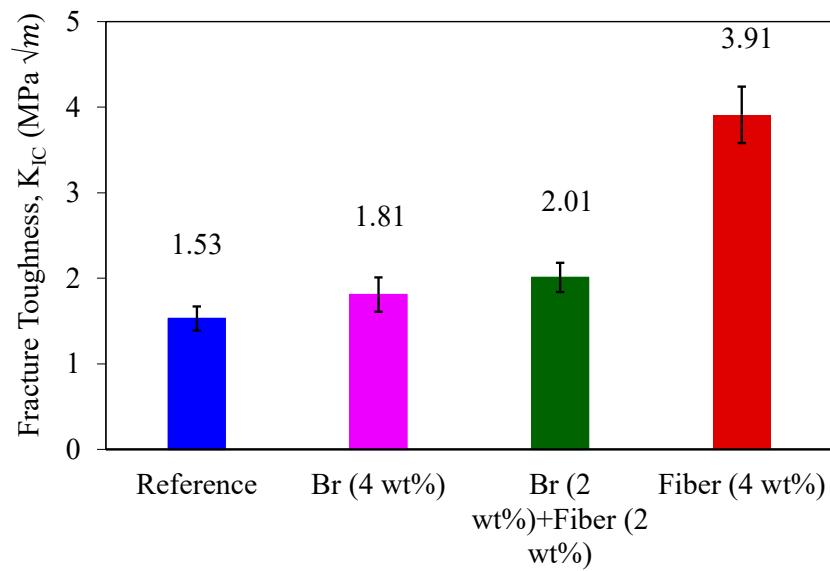
Table 4. Maximum load and displacement at the final failure point for SCB samples.

Sample No.	Maximum Load, P (N)	Displacement at Final Failure, δ (mm)
Reference (PC with no additives)	5119	0.54
Br (2%)	6174	0.70
Br (1%) and Fiber (1%)	8289	1.07
Fiber (2%)	6865	2.06
Br (4%)	5706	0.60
Br (2%) and Fiber (2%)	6941	2.15
Fiber (4%)	12,222	3.65
Br (8%)	7183	0.90
Br (4%) and Fiber (4%)	8571	2.04
Fiber (8%)	10,224	3.089

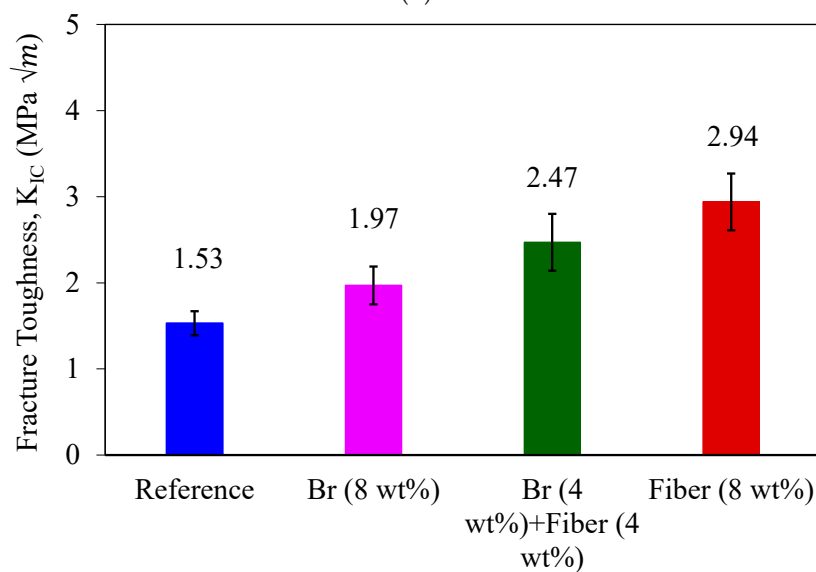
In Figure 11, the average fracture toughness values, determined using Equation (3), are presented. According to the obtained results, the mode I fracture toughness increased by 32% with the addition of 2 wt% brass chips, while 1 wt% glass fibers + 1 wt% brass chips improved the fracture energy by 53%. Also, the addition of 4 wt% glass fibers increased the fracture toughness by 156%. Furthermore, the incorporation of 4 wt% glass fibers along with 4 wt% brass chips resulted in a remarkable 61% increase in fracture toughness. Nevertheless, the most exceptional performance was achieved when solely glass fibers were introduced to the PC samples, yielding an impressive 92% improvement in fracture energy. Based on the experimental findings, it can be deduced that the addition of glass fibers exerts the most significant influence on the fracture energy of the tested PCs. Notably, the introduction of 4 wt% glass fibers demonstrates the most substantial effect in enhancing the mode I fracture toughness of the tested concretes.



(a)



(b)



(c)

Figure 11. Average mode I fracture toughness of SCB specimens in the states of (a) 2 wt%, (b) 4 wt%, and (c) 8 wt% under fracture test.

In Figure 12, the fracture surface of SCB specimens cracked under mode I loading is presented. The path of crack propagation observed in both strength and fracture tests originates from within the aggregates and at the interface between the aggregate and resin. The predominant failure mechanism identified in this study encompasses aggregate breakage, as well as adhesive and aggregate debonding. In fact, in samples without fillers, the predominant mechanism that inhibits crack growth or damage is aggregate fracture and debonding between the aggregate and adhesive. However, in samples containing fillers, in addition to these two mechanisms, the presence of fibers or metal chips can further impede crack growth and lead to multiple site cracking within the sample (see Figure 8).

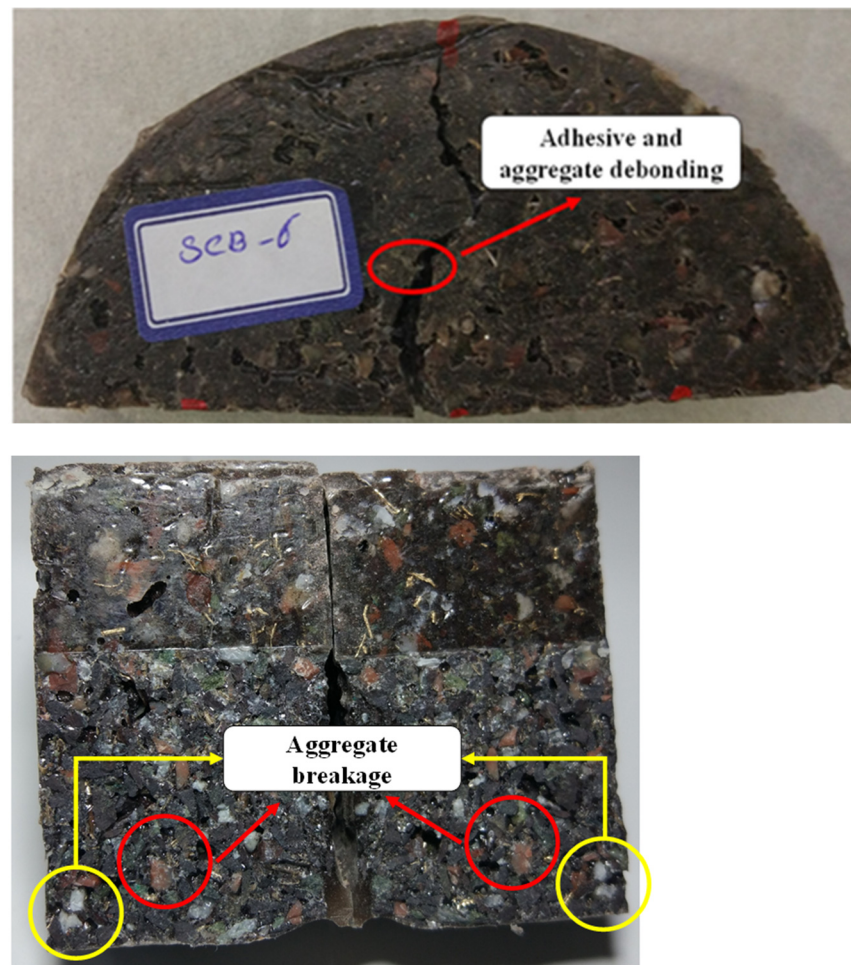


Figure 12. Fracture surface of SCB specimens with a central crack.

4. Conclusions

In this study, the experimental investigation aimed to assess the influence of metal chips and glass fibers as fillers on the mode I fracture toughness, tensile strength, and energy absorption until failure of the PC material. SCB samples were fabricated using epoxy resin and waste mineral aggregates, with variations including 10 groups without filler and incorporating different weight ratios of various filler types, such as glass fibers, discarded metal chips, and various combinations of these materials. Quasi-static 3PB tests were conducted on samples without pre-cracks to determine the tensile strength of the SCB samples. The experimental results found that:

- The addition of fillers had minimal influence on tensile strength.
- The addition of 4 wt% glass fibers increased the energy absorption by 953%.

- Glass fibers have more impact on the mechanical response of the tested PCs compared to brass chips, and the inclusion of 8 wt% glass fibers substantially improved (by 92%) the resistance of the PC components to crack propagation.
- At lower weight ratios, a combination of brass chips and glass fibers could enhance the fracture response of the tested PCs.
- In unfilled samples, the main mechanism preventing crack propagation is aggregate fracture and the separation of the aggregate from the adhesive. Yet, in filled samples, alongside these mechanisms, the presence of fibers or metal chips adds an extra barrier to crack advancement, resulting in multiple-site cracking within the sample.

Author Contributions: Methodology, M.S.-T. and F.S.; Validation, A.A.-S.; Investigation, M.S.-T. and A.Z.-B.; Resources, F.S. and R.J.C.C.; Writing—original draft, M.S.-T. and A.Z.-B.; Writing—review & editing, A.A.-S., R.J.C.C. and L.F.M.d.S.; Supervision, L.F.M.d.S. All authors have read and agreed to the published version of the manuscript.

Funding: This research received no external funding.

Institutional Review Board Statement: Not applicable.

Informed Consent Statement: Not applicable.

Data Availability Statement: No new data were created or analyzed in this study. Data sharing is not applicable to this article.

Conflicts of Interest: The authors declare no conflict of interest.

References

1. Fang, H.; Su, Z.; Li, X.; Wang, F.; Fu, Y. Interfacial bond performance between self-expansion polymer and concrete. *Constr. Build. Mater.* **2021**, *270*, 121459. [[CrossRef](#)]
2. Güler, Ö.; Cacim, N.N.; Evin, E.; Yahia, I.S. The synergistic effect of CNTs-polymeric surfactant on the properties of concrete nanocomposites: Comparative study. *J. Compos. Mater.* **2021**, *55*, 1371–1384. [[CrossRef](#)]
3. Islam, S.M.; Hussain, R.R.; Morshed, M.A.Z. Fiber-reinforced concrete incorporating locally available natural fibers in normal-and high-strength concrete and a performance analysis with steel fiber-reinforced composite concrete. *J. Compos. Mater.* **2012**, *46*, 111–122. [[CrossRef](#)]
4. Karamzadeh, N.S.; Aliha, M.; Karimi, H.R. Investigation of the effect of components on tensile strength and mode-I fracture toughness of polymer concrete. *Arab. J. Geosci.* **2022**, *15*, 1213. [[CrossRef](#)]
5. Reza Karimi, H.; Aliha, M. Statistical assessment on relationship between fracture parameters of plain and fiber reinforced polymer concrete materials. *Compos. Commun.* **2021**, *28*, 100969. [[CrossRef](#)]
6. Alhazmi, H.; Shah, S.A.R.; Anwar, M.K.; Raza, A.; Ullah, M.K.; Iqbal, F. Utilization of polymer concrete composites for a circular economy: A comparative review for assessment of recycling and waste utilization. *Polymers* **2021**, *13*, 2135. [[CrossRef](#)] [[PubMed](#)]
7. Aliha, M.; Imani, D.; Salehi, S.; Shojaei, M.; Abedi, M. Mixture optimization of epoxy base concrete for achieving highest fracture toughness and fracture energy values using Taguchi method. *Compos. Commun.* **2022**, *32*, 101150. [[CrossRef](#)]
8. Józefiak, K.; Michalczyk, R. Prediction of structural performance of vinyl ester polymer concrete using FEM elasto-plastic model. *Materials* **2020**, *13*, 4034. [[CrossRef](#)] [[PubMed](#)]
9. Heidarneshad, F.; Jafari, K.; Ozbakkaloglu, T. Effect of polymer content and temperature on mechanical properties of lightweight polymer concrete. *Constr. Build. Mater.* **2020**, *260*, 119853. [[CrossRef](#)]
10. Wang, J.; Dai, Q.; Guo, S.; Si, R. Mechanical and durability performance evaluation of crumb rubber-modified epoxy polymer concrete overlays. *Constr. Build. Mater.* **2019**, *203*, 469–480. [[CrossRef](#)]
11. Aliha, M.; Heidari-Rarani, M.; Shokrieh, M.; Ayatollahi, M. Experimental determination of tensile strength and K (IC) of polymer concretes using semi-circular bend (SCB) specimens. *Struct. Eng., Mech.* **2012**, *43*, 823. [[CrossRef](#)]
12. Ohama, Y.; Ramachandran, V. Polymer-modified mortars and concretes. In *Concrete Admixtures Handbook*; Elsevier: Amsterdam, The Netherlands, 1996; pp. 558–656.
13. Jafari, K.; Tabatabaeian, M.; Joshaghani, A.; Ozbakkaloglu, T. Optimizing the mixture design of polymer concrete: An experimental investigation. *Constr. Build. Mater.* **2018**, *167*, 185–196. [[CrossRef](#)]
14. Ren, S.; Hu, X. Fatigue properties and its prediction of polymer concrete for the repair of asphalt pavements. *Polymers* **2022**, *14*, 2941. [[CrossRef](#)] [[PubMed](#)]
15. Maldonado-García, B.; Pal, A.K.; Misra, M.; Gregori, S.; Mohanty, A.K. Sustainable 3D printed composites from recycled ocean plastics and pyrolyzed soy-hulls: Optimization of printing parameters, performance studies and prototypes development. *Compos. Part C Open Access* **2021**, *6*, 100197. [[CrossRef](#)]

16. Lewis, R.; Weldekidan, H.; Rodriguez, A.U.; Mohanty, A.K.; Mielewski, D.F.; Misra, M. Design and Engineering of Sustainable Biocomposites from Ocean-Recycled Polypropylene-based Polyolefins and Almond Shell and hull. *Compos. Part C Open Access* **2023**, *12*, 100373. [[CrossRef](#)]
17. Davies, P.; Le Gall, M.; Niu, Z.; Catarino, A.; De Witte, Y.; Everaert, G.; Dhakal, H.; Park, C.; Demeyer, E. Recycling and ecotoxicity of flax/PLA composites: Influence of seawater aging. *Compos. Part C Open Access* **2023**, *12*, 100379. [[CrossRef](#)]
18. Azarhoosh, A.; Koohmishi, M.; Moghadas Nejad, F. Evaluation of fatigue cracking of hot-mix asphalts containing recycled concrete aggregates coated with waste plastic bottles using thermodynamic parameters. *J. Adhes.* **2022**, *98*, 1076–1096. [[CrossRef](#)]
19. Grilli, V.; Virgili, A.; Graziani, A. Evaluation of complex modulus and fatigue properties of cold recycled material mixtures using small-scale specimens. *Road Mater. Pavement Des.* **2023**, *25*, 1–16. [[CrossRef](#)]
20. Joshi, R.; Bajpai, P.K.; Mukhopadhyay, S. Processing and performance evaluation of agro wastes reinforced bio-based epoxy hybrid composites. *Proc. Inst. Mech. Eng. Part L* **2023**, *237*, 482–499. [[CrossRef](#)]
21. Sankar, I.; Siva, I. The synergy of fiber surface treatment and nanoclay on the static mechanical and tribological behaviors of Palmyra fruit fiber/Montmorillonite nanoclay reinforced polyester hybrid composites. *Proc. Inst. Mech. Eng. Part L* **2023**, *237*, 122–130. [[CrossRef](#)]
22. Hameed, A.M.; Hamza, M.T. Characteristics of polymer concrete produced from wasted construction materials. *Energy Procedia* **2019**, *157*, 43–50. [[CrossRef](#)]
23. Rokbi, M.; Baali, B.; Rahmouni, Z.; Latelli, H. Mechanical properties of polymer concrete made with jute fabric and waste marble powder at various woven orientations. *Int. J. Environ. Sci. Technol.* **2019**, *16*, 5087–5094. [[CrossRef](#)]
24. Son, S.-W.; Yeon, J.H. Mechanical properties of acrylic polymer concrete containing methacrylic acid as an additive. *Constr. Build. Mater.* **2012**, *37*, 669–679. [[CrossRef](#)]
25. D'Alessandro, F.; Asdrubali, F.; Baldinelli, G. Multi-parametric characterization of a sustainable lightweight concrete containing polymers derived from electric wires. *Constr. Build. Mater.* **2014**, *68*, 277–284. [[CrossRef](#)]
26. Kou, S.-C.; Poon, C.-S. A novel polymer concrete made with recycled glass aggregates, fly ash and metakaolin. *Constr. Build. Mater.* **2013**, *41*, 146–151. [[CrossRef](#)]
27. Teixeira, E.R.; Camões, A.; Branco, F. Valorisation of wood fly ash on concrete. *Resour. Conserv. Recycl.* **2019**, *145*, 292–310. [[CrossRef](#)]
28. Bulut, H.A.; Şahin, R. A study on mechanical properties of polymer concrete containing electronic plastic waste. *Compos. Struct.* **2017**, *178*, 50–62. [[CrossRef](#)]
29. Heidari-Rarani, M.; Aliha, M.; Shokrieh, M.; Ayatollahi, M. Mechanical durability of an optimized polymer concrete under various thermal cyclic loadings—An experimental study. *Constr. Build. Mater.* **2014**, *64*, 308–315. [[CrossRef](#)]
30. Aliha, M.; reza Karimi, H.; Abedi, M. The role of mix design and short glass fiber content on mode-I cracking characteristics of polymer concrete. *Constr. Build. Mater.* **2022**, *317*, 126139. [[CrossRef](#)]
31. Asdollah-Tabar, M.; Heidari-Rarani, M.; Aliha, M. The effect of recycled PET bottles on the fracture toughness of polymer concrete. *Compos. Commun.* **2021**, *25*, 100684. [[CrossRef](#)]
32. Heidari-Rarani, M.; Bashandeh-Khodaei-Naeini, K. Micromechanics based damage model for predicting compression behavior of polymer concretes. *Mech. Mater.* **2018**, *117*, 126–136. [[CrossRef](#)]
33. Salamat-Talab, M.; Akhavan-Safar, A.; Zeinolabedin-Beygi, A.; Carbas, R.J.; da Silva, L.F. Effect of Through-the-Thickness Delamination Position on the R-Curve Behavior of Plain-Woven ENF Specimens. *Materials* **2023**, *16*, 1811. [[CrossRef](#)] [[PubMed](#)]
34. Akhavan-Safar, A.; Salamat-Talab, M.; Delzendehrooy, F.; Zeinolabedin-Beygi, A.; da Silva, L. Effects of natural date palm tree fibres on mode II fracture energy of E-glass/epoxy plain-woven laminated composites. *J. Braz. Soc. Mech. Sci. Eng.* **2022**, *44*, 457. [[CrossRef](#)]
35. Safari, M.; de Sousa, R.A.; Salamat-Talab, M.; Joudaki, J.; Ghanbari, D.; Bakhtiari, A. Mechanical properties of green synthesized graphene nano-composite samples. *Appl. Sci.* **2021**, *11*, 4846. [[CrossRef](#)]
36. Salamat-Talab, M.; Safaei, S.; Soltani, F.; Akhavan-Safar, A.; da Silva, L.F. Fracture Toughness Analysis of Polymer Concretes Made by Waste Mineral Aggregates and Enhanced with Glass Fibers and Metal Chips. In Proceedings of the 1st International Conference on Mechanics of Solids, Porto, Portugal, 3–4 November 2022; Springer: Berlin/Heidelberg, Germany, 2022; pp. 33–45.
37. Tahmasbi, V.; Zeinolabedin-Beygi, A.; Elahi, S.H.; Ashtiani, M.A. Statistical modeling, optimization and sensitivity analysis of dried turning of aluminum bronze alloy. *Sādhanā* **2022**, *47*, 232. [[CrossRef](#)]
38. Ghabezi, P.; Farahani, M. Composite adhesive-bonded joint reinforcement by incorporation of nano-alumina particles. *J. Comput. Appl. Mech.* **2016**, *47*, 231–239.
39. Aliha, M.; Pour, P.J.H. Fracture resistance study for hot mix asphalt mixture under out of plane sliding mode. *Eng. Fract. Mech.* **2020**, *238*, 107230. [[CrossRef](#)]
40. Najjar, S.; Moghaddam, A.M.; Sahaf, A.; Aliha, M. Low temperature fracture resistance of cement emulsified asphalt mortar under mixed mode I/III loading. *Theor. Appl. Fract. Mech.* **2020**, *110*, 102800. [[CrossRef](#)]
41. Fakhri, M.; Siyadati, S.A.; Aliha, M. Impact of freeze–thaw cycles on low temperature mixed mode I/II cracking properties of water saturated hot mix asphalt: An experimental study. *Constr. Build. Mater.* **2020**, *261*, 119939. [[CrossRef](#)]
42. Mubarak, M.; Abd-Elhady, A.A.; Sallam, H. Mixed mode fracture toughness of recycled tire rubber-filled concrete for airfield rigid pavements. *Int. J. Pavement Res. Technol.* **2013**, *6*, 8–14.

43. Seitl, S.; Miarka, P. Evaluation of mixed mode I/II fracture toughness of C 50/60 from Brazilian disc test. *Frat. Integrità Strutt.* **2017**, *11*, 119–127. [[CrossRef](#)]
44. Reis, J.; Ferreira, A. The effects of atmospheric exposure on the fracture properties of polymer concrete. *Build. Environ.* **2006**, *41*, 262–267. [[CrossRef](#)]
45. Akhavan-Safar, A.; Salamat-Talab, M.; Delzendehrooy, F.; Barbosa, A.; da Silva, L. Mode II fracture energy of laminated composites enhanced with micro-cork particles. *J. Braz. Soc. Mech. Sci. Eng.* **2021**, *43*, 490. [[CrossRef](#)]
46. Ayatollahi, M.; Aliha, M. Wide range data for crack tip parameters in two disc-type specimens under mixed mode loading. *Comput. Mater. Sci.* **2007**, *38*, 660–670. [[CrossRef](#)]
47. Shokrieh, M.M.; Saeedi, A.; Chitsazzadeh, M. Mechanical properties of multi-walled carbon nanotube/polyester nanocomposites. *J. Nanostruct. Chem.* **2013**, *3*, 20. [[CrossRef](#)]

Disclaimer/Publisher’s Note: The statements, opinions and data contained in all publications are solely those of the individual author(s) and contributor(s) and not of MDPI and/or the editor(s). MDPI and/or the editor(s) disclaim responsibility for any injury to people or property resulting from any ideas, methods, instructions or products referred to in the content.